Selected-Control Hydrothermal Synthesis of γ-MnO_2 3D Nanostructures

Changzheng Wu, Yi Xie,* Dong Wang, Jun Yang, and Tanwei Li

Structure Research Laboratory, Department of Chemistry, University of Science and Technology of China, Hefei, Anhui 230026, P. R. China

Received: June 4, 2003; In Final Form: September 25, 2003

Highly uniform γ-MnO_2 3D urchinlike and sisallike nanostructures have been successfully prepared by a common hydrothermal method based on the reaction between $MnSO_4$ and $KBrO_3$. Reaction temperature and the additives of the polymers play an important role in influencing the morphologies of the as-obtained products. These urchinlike and sisallike nanostructures, which own the highly specific area on the surface of the particles may provide more possibility to give an ideal host material for the insertion and extraction of lithium ions, to realize region-dependent surface reactivity, and to act as molecular sieves.

Introduction

Because different morphologies and crystallographic forms are generally believed to be responsible for their properties, how to control the anisotropic inorganic materials at the mesoscopic level is one of the most challenging issues presently faced by synthetic chemists. Recently, research on nanostructures is expanding rapidly into the assembly of nanoparticles in two-dimensional (2D) and three-dimensional (3D) ordered superstructures.[1] Much effort has been made in the fabrication of patterns of well-arranged nanocrystallites, especially the arrangement of one-dimensional nanotubes and nanorods because of their interesting physical properties and potential applications in many areas.[2] Due to their anisotropic structure, the oriented growth of nanorods and nanowires is difficult and usually requires solid templates, such as porous alumina, polymer nanotubes, and patterned catalysts, to control the direct growth.[3] However, the introduction of templates and substrates introduces heterogeneous impurities and increases the production cost, which may restrict the wide development of researches and applications. Thus how to develop facile, mild, easily-controlled, and template-free methods to create novel patterns on self-generated homogeneous substrates is of great significance.

Many polymorphic forms of manganese dioxide, such as α-, β-, γ-, and δ-type, have drawn considerable attention because of their distinctive properties and now are widely used as catalysts and electrode materials in Li/MnO_2 batteries.[4] Moreover, manganese dioxides with well-controlled dimensionality, size, and crystal structure have also been regarded as critical factors that may bring some novel and unexpected properties, for example, isotropic or anisotropic behavior and region-dependent surface reactivity. Therefore, development of the morphologically controllable synthesis of MnO_2 nanoparticles is urgently important to answer the demand for exploring the potentials of MnO_2. Over the past few years, remarkable process has been made in the synthesis of MnO_2 with different morphologies and different crystallographic forms. α- and Tokorokite-type MnO_2 were found to have fiber or needle morphologies.[5] Li and co-workers reported the hydrothermal preparation of α-MnO_2 nanowires and β-MnO_2 nanorods by oxidizing $MnSO_4$ in $KMnO_4$ and $K_2S_2O_8$, respectively.[6] Very recently, our group synthesized γ-MnO_2 nanowires through a coordination-polymer-precursor route.[7] However, how to control both the morphology and the phase of γ-MnO_2 nanowires by the direct reaction route is still unsolved,[6,7] and how to accomplish highly oriented growth of γ-MnO_2 nanostructures remains a key research challenge.

Herein, we demonstrate a facile selected-control hydrothermal method to synthesize highly pure uniform urchinlike 3D γ-MnO_2 nanostructures (in these structures, nanorods or nanowires grow radially from the core particles) via the direct reaction between only $MnSO_4$ and $KBrO_3$. When the polymers (such as poly(ethylene glycol)-20000 (PEG-20000), poly(ethylene glycol)-400 (PEG-400), and poly(vinylpyrrolidone)-K30 (PVP-K30, average MW 58 000)) were introduced into this system, the sisallike 3D nanostructures (in these structures, broad leaves grow radially from the core particles) can be obtained. As we all know, up to now, there has been no report on selectively controlled 3D morphologies (urchinlike nanostructures, sisallike nanostructures) for γ-MnO_2 under mild conditions. And the urchinlike and sisallike nanostructures, which own the highly specific area on the surface of the particles, may provide more possibility to give an ideal host material for the insertion and extraction of lithium ions, to realize region-dependent surface reactivity, and to act as molecular sieves.

Experimental Section

The chemical reaction that we employed for synthesis of the γ-MnO_2 3D nanostructures can be formulated as

$$5MnSO_4 + 2KBrO_3 + 4H_2O \rightarrow 5\gamma\text{-}MnO_2 + Br_2 + K_2SO_4 + 4H_2O$$

To prepare urchinlike nanostructures, a 50 mL aqueous solution containing 2 mmol of $MnSO_4$ and 1 mmol of $KBrO_3$ was put in a conical flask and was stirred with a magnetic stirrer until a transparent solution was obtained. The solution was then transferred into a 60 mL Teflon-lined stainless steel autoclave, sealed, and was slowly heated to 110 or 130 °C at 1 °C/min. And then the autoclave was maintained at 130 °C for 16 h.

To prepare γ-MnO_2 sisallike nanostructures, 0.4 g of PEG (or 0.6 g of PVP) was introduced, and the autoclave was heated to 110 °C (or 90 °C for PVP) and maintained for 16 h.

* Corresponding author. Tel: 86-551-3603987. Fax: 86-551-3603987. E-mail: yxielab@ustc.edu.cn.

10.1021/jp035567r CCC: $25.00
Published on Web 11/14/2003

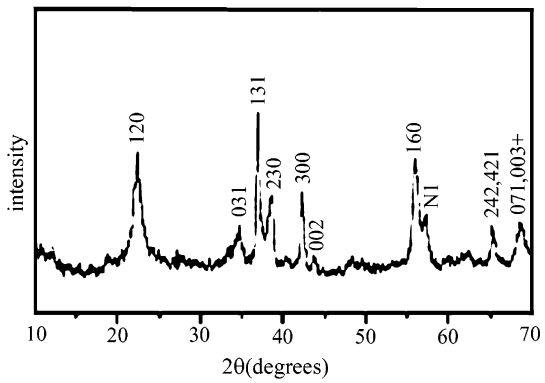

Figure 1. XRD pattern of the as-obtained γ-MnO_2 3D nanostructures obtained by the direct reaction between $MnSO_4$ and $KBrO_3$ at 110 °C.

After the reaction completed, the resulting black solid product was filtered, washed with distilled water and absolute ethanol to remove byproducts, and then dried at 60 °C in air. The obtained black powders were collected for the following characterization.

The samples were characterized by X-ray powder diffraction (XRD) pattern with a Japan Rigaku D/max rA X-ray diffractometer equipped with graphite monochromatized high-intensity Cu Kα radiation (λ = 1.541 78 Å). The transmission electron microscopy (TEM) images were performed with a Hitachi model H-800 instrument with a tungsten filament, using an accelerating voltage of 200 kV. The field emission scanning electron microscopy (FE-SEM) images were taken on a JEOL JSM-6700F SEM. The electron diffraction (ED) patterns and high-resolution transmission electron microscopy (HRTEM) images were carried out on a JEOL-2010 TEM at an acceleration voltage of 200 kV. IR absorption spectra were performed with a Nicolet FT-IR-170SX spectrometer in the range of 250 ± 450 cm^{-1} at room temperature with the sample in a KBr disk.

Results and Discussion

XRD Patterns of the Products. X-ray powder diffraction (XRD) patterns reveal the phase and purity of as-obtained products. Figure 1 shows a typical XRD pattern of γ-MnO_2 urchinlike nanostructures obtained by the direct reaction between $MnSO_4$ and $KBrO_3$ at 110 °C. All of the reflection peaks can be readily indexed to pure orthorhombic γ-MnO_2 (JCPDS card 14-644, a = 6.36 Å, b = 10.15 Å, c = 4.09 Å). Similar XRD patterns were obtained from the sisallike nanostructures and other product of the comparison experiment, all of which exhibited orthorhombic γ-MnO_2. No characteristic peaks are observed for other impurities such as α-, β-, and δ-MnO_2.

The Morphology of the Obtained Product. The urchinlike nanostructures were obtained through the direct reaction between $MnSO_4$ and $KBrO_3$ at 110 and 130 °C. Shown in Figure 2 is the as-obtained urchinlike nanostructures synthesized at 110 °C. The panoramic morphology of the product was obtained by the field emission scanning electron microscopy (FE-SEM), in which the solid sample was mounted on a copper mesh without any dispersion treatment, indicating that all samples (Figure 2A) are uniform urchinlike nanostructures with diameter of 4−10 μm, and the proportion of the urchinlike nanostructures in the whole sample is above 85%. Careful observation (Figure 2B,C) can find that the urchinlike nanostructures consist of uniform nanorods with the diameter of 40−100 nm and length up to 1 μm. With a raised temperature of 130 °C, we obtained nanowires with high aspect ratio grown radially from the core particles. As shown in Figure 3A, these nanowires have uniform diameter ranging from 20 to 50 nm with length up to 10 μm. More details about the structure of as-obtained nanowires were investigated by the electron diffraction (ED) patterns (inset image in Figure 3B) and high-resolution transmission electron microscopy (HRTEM) (Figure 3B), which indicate that they are structurally uniform monocrystalline grown along [002] direction.

It is well-known that using a polymer-assisted reaction to control the nucleation and growth is a simple but effective way, and different environments for nucleation and growth of products will be created and will affect the morphology of the precipitations by using different polymers with various molecular weights. For the case of γ-MnO_2, sisallike nanostructures can be synthesized with the addition of polymer. Figure 4A−C shows the as-obtained sisallike nanostructures synthesized with the addition of PEG-20000 at 110 °C. The panoramic morphology (Figure 4A) of the obtained product shows that the as-obtained products consist of highly uniform spherical aggregates with a diameter of 5−6 μm that consist of acicular crystallites radiating from the center (Figure 4B) and these uniform acicular crystallites are approximately 3 μm long by 200−400 nm wide (Figure 4C). However, when low molecular weight polymers (PEG-400) were introduced into this system, the coexistence of the broad leaves and high aspect ratio nanowires grown from the particles were obtained as shown in Figure 4D and its magnified image Figure 4E. The use of another high molecular weight polymer (PVP-K30, average MW 58 000) led to the uniform broad leaves (Figure 4E,F) similar to those obtained by PEG-20000 (Figure 4A−C), implying that molecular weight plays an important role in the formation of broad-leave structures.

Formation Mechanism of the As-Obtained Sisallike Nanostructures. To study the influence of the polymer, PEG-20000 was taken as an example. Both IR absorption spectrum (Figure 5) and TEM image (Figure 6A,B) indicate that there is a strong interaction between the surfaces of the MnO_2 nanoparticles and PEG-20000, although the exact bonding geometry and the nature of selectivity between different crystallographic planes are still unclear. To investigate the formation process of the γ-MnO_2 sisallike nanostructures, the IR absorption spectrum of the pure PEG-20000 was measured (Figure 5A). In the IR region, the

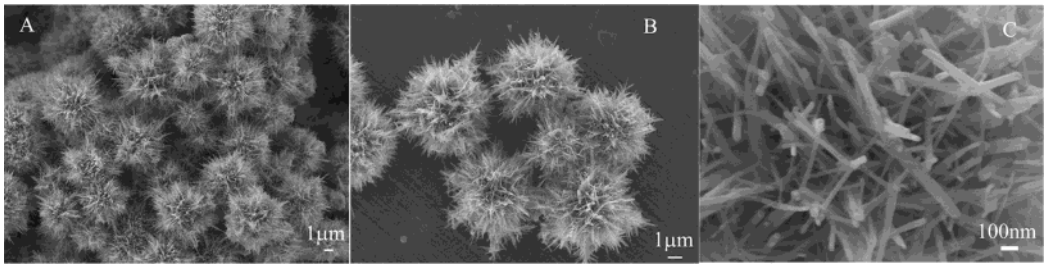

Figure 2. FE-SEM images of obtained urchinlike nanostructures at 110 °C: the panoramic morphologies (A), low magnification (B), and high magnification images (C).

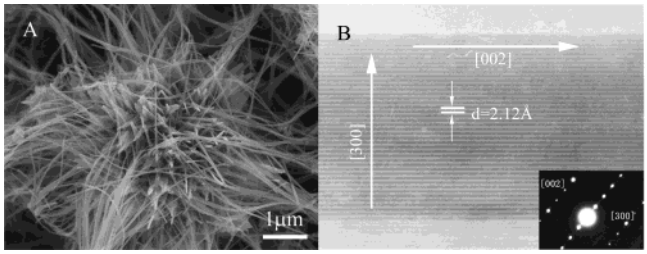

Figure 3. (A) FE-SEM image of the as-obtained urchinlike nanostructures radiated with high aspect ratio nanowires at 130 °C and (B) HRTEM image of the γ-MnO_2 nanowires covered on urchinlike nanostructures (inset is its corresponding ED pattern).

absorption peaks at 1110 and 2896 cm^{-1} are the −O− and C−H stretching vibrations in PEG-20000, respectively.[8] By comparison, the obtained precipitates with reaction times of 2, 4, and 12 h were also determined by IR spectra. It was found that the absorption peeks of the −O− and C−H stretching vibration in PEG gradually disappeared. On the other hand, the absorption peaks at 475−710 cm^{-1}, which were assigned to the Mn−O stretching vibration of γ-MnO_2,[9] appeared and their intensity increased with increasing reaction time. These characterization results reveal that the dissociation of the coordination polymer and the formation of γ-MnO_2 sisallike nanostructures occurred at the same time, indicating that polymer additive might play a certain role in the formation of the broad leaves. TEM image clearly shows that the spherical particle was covered tightly by the polymers, which provides a further evidence for the function of the polymer (Figure 6B).

Detailed TEM study on the formation of sisallike nanostrucrtures was shown in Figure 6, from which one can clearly see that the polymer covered on the MnO_2 particles was thinner as the MnO_2 particles grew larger. When the particle was so large that the polymer cannot cover the aggregation particle tightly, the anisotropic growth will occur and some initial broad leaf structures will form on the edge of the particles as shown in Figure 6E, from which one can see that there exist no curling structures. It is worth noting that the intermediate structure as shown in Figure 6D is similar to the aggregated particle as shown in Figure 7A, which was obtained by the direct reaction at 110 °C. These two similar structures lead to two different results: the former results in the formation of sisallike nanostructures; however, the latter one leads to urchinlike nanostructures. We believe that this difference may result from the influence of the polymers. The lamellar structures grown from the aggregated particles are stable because of the assistance of the organic additives.[10] These as-obtained lamellar structures will grow longer and thicker during the following hydrothermal process, and finally the sisallike nanostructures formed. However, when the low molecular weight polymer (such as PEG-400) was introduced, the coexistence of broad leaves and some nanowires grown from the core particles could be seen from the products. The exact mechanism for the formation of such morphology resulting from the additive of PEG-400 is still under investigation; however, it appears to be related to the weaker interaction between the surface of the aggregated particles and the low molecular weight polymers due to the higher moving rate and moving range of low molecular weight polymers. Thus, some of the lamellar structures will curl and collapse into nanowires (shown in Figure 4D,E) without the effective influence of coordination effect. Moreover, the additive of PVP may provide another proof to confirm the above mechanism, in that the pure broad leaves grow radially from the core particles as shown in Figure 4E.

Formation Mechanism of the As-Obtained Urchinlike Nanostructures. TEM study on sisallike nanostructures clearly indicates polymers play a crucial role in the formation of broad leaves on the aggregated particles. In fact, the formation mechanism of the urchinlike nanostructures is similar to that of the sisallike nanostructures in the aggregation process, and then the nanorods and nanowires were produced on the aggregated particle core as a result of the "rolling-broken-growth" (RGB) process because the polymers were absent. An intermediate sample was obtained in an experiment at 110 °C with a short reaction time of 1 h and was investigated by TEM. As shown in Figure 7A, one can clearly see the aggregated particle core, just like that in sisallike nanostructures. Careful observation of the core particle can find that there are some thin flakes (Figure 7B) and curling structures (Figure 7C) formed on the edge of the accumulated particle, which may serve as a powerful proof that a "rolling-broken-growth"(RBG) happened and lead to the initial formation of the nanorods and nanowires in the urchinlike nanostructures. Moreover, the thin flakes structures were grown out from the aggregated particles, indicating that the aggregation process may occur before the formation of the lamellar structures. At the beginning of the reaction, the MnO_x units will appear first in the solution, and these units tend to aggregate with each other to form the aggregated particles. Through a condensation reaction, they will form thin flakes[11] on the edge of the aggregated particles (Figure

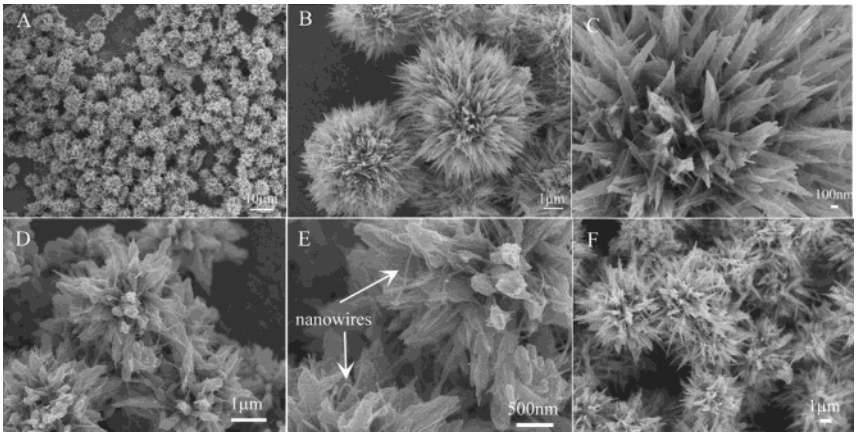

Figure 4. FE-SEM images: (A−C) the panoramic morphologies, low magnification, and high magnification images of the obtained sisallike nanostructures with the addition of PEG-20000, respectively; (D−E) low magnification and high magnification images of the as-obtained sisallike nanostructures with the addition of PEG-400, showing that the coexistence of the broad leaves and some nanowires grown from the core particles; (F) the obtained sisallike nanostructures with the addition of PVP-K30.

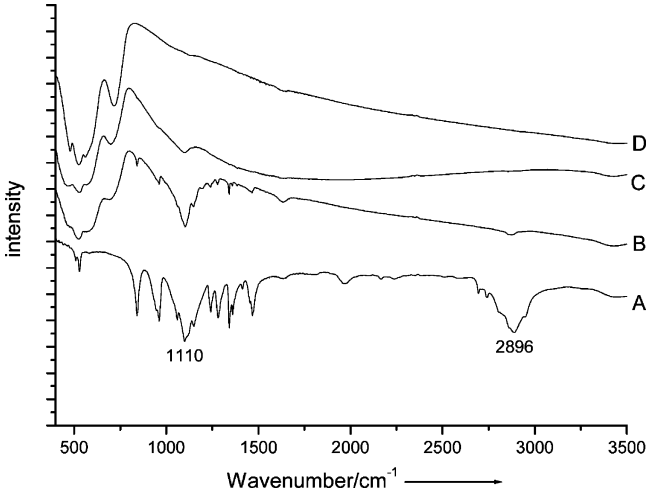

Figure 5. IR spectrum study of the function of PEG-20000: (A) PEG-20000; (B−D) precipitates after reaction for 2, 4, and 12 h, respectively.

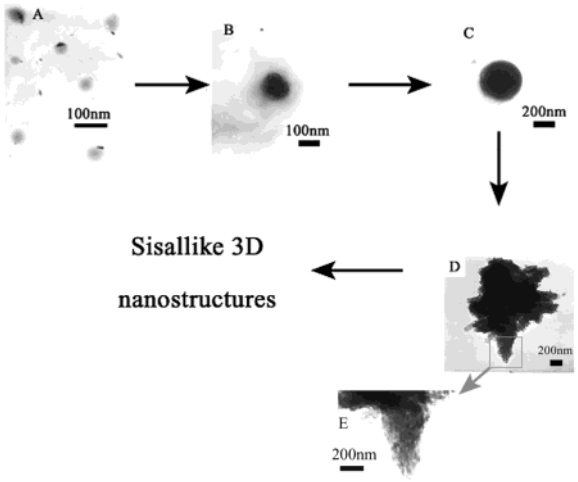

Figure 6. TEM study on the formation mechanism of the sisallike 3D nanostructures. At the beginning (panel A), the initial nuclei were very small, while the relatively thicker polymer was tangled seriously. Thus the newly formed particles can hardly be seen under the heavy cover as shown in panel A. Then the particle grew bigger (panel B), and the polymer molecule became loose and sparse to accommodate the grown particle. When the particle grew large enough, the polymer can hardly cover the particle (panel C) and formed only an obscure ring in the TEM image. In panel D, the particle was too large to be covered completely by the polymer layer and some broad leaves grew out from the core particle. Panel E shows the magnified image of the rectangle part in image D.

7B). The thin flakes tend to curl (Figure 7C) under the elevated temperature and pressure and will collapse into nanorods without any assistance via "rolling-broken-growth" (RGB) process. During the following hydrothermal process, the shorter ones may redissolve into the solution phase, and the longer ones grow into much longer ones, similar to the formation of Se[12] and Ag[13] nanowires.

It is worth noting that the aspect ratios of the final products are determined by the anisotropic growth of the corresponding crystal structures. We believe that the formation of γ-MnO_2 nanowires is actually the outward embodiment of the nature of the initial crystal structure. Although γ-MnO_2 consists of a random arrangement of single and double chains of MnO_6 octahedra[14] (Figure 8A), it is found that in γ-MnO_2 each Mn cation is connected to three adjacent cations through oxygen anions to build up distorted Mn hexagonal units in layers, which are composed of Mn cation frameworks shown in Figure 8B.[7]

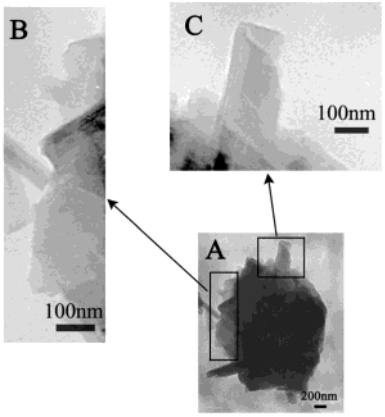

Figure 7. The TEM image (A) of the intermediate in the formation of urchinlike nanostructures and (B,C) the images with higher magnification of image A, from which one can find the lamellar (B) and curling structures (C).

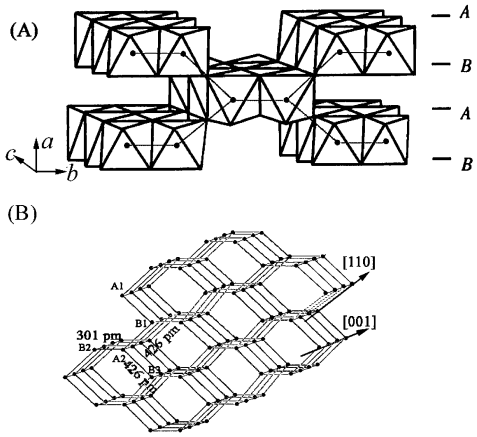

Figure 8. (A) The structure of γ-MnO_2 with a random arrangement of single and double chains of MnO_6 octahedra.[7] The dots represent the positions of Mn cations. In panel B, the framework of the Mn cations in the γ-MnO_2 crystal lattice is shown, from which the chainlike building blocks can be seen along [001] direction.

Along the [001] direction, the chainlike building blocks can be clearly seen. And the anisotropic nature of these building blocks in the crystal structure plays a crucial role in the formation of low-dimension nanomaterials, which provides a possibility for the formation of γ-MnO_2 nanowires in the soft solution processing strategy. As for the influence of temperature, it is generally believed that a higher temperature is preferable for the anisotropic growth of crystal and results in the product with high aspect ratio grown from the core particles (Figure 3A); meanwhile, at a lower temperature of 110 °C, shorter nanorods will be obtained as shown in Figure 2.

Conclusions

In conclusion, we have developed a facile selected-control hydrothermal method to synthesize highly uniform urchinlike γ-MnO_2 nanostructures via the mild and the direct reaction between $MnSO_4$ and $KBrO_3$. When the polymers (such as PEG and PVP) were introduced into this system, the sisallike nanostructures with narrow or broad leaves can be obtained via the addition of polymers with different molecular weight, respectively. Possible mechanism was proposed to elucidate their formation. These urchinlike and sisallike nanostructures, which own the highly specific area on the surface of the particles, may bring some novel and unexpected properties, for example, molecular sieves and catalysts, especially for the Li/MnO_2

batteries. Further work is under way to study the properties of these novel 3D nanostructures and the possibility of synthesizing other 3D nanostructures.

Acknowledgment. This work was supported by National Natural Science Foundation of China, Chinese Ministry of Education, and Chinese Academy of Science. The authors thank Prof. Shuyuan Zhang and Prof. Fanqing Li for technical assistance in HRTEM and FE-SEM experiments, respectively.

References and Notes

(1) (a) Yonezawa, T.; Onoue, S.; Kimizuka, N. *Adv. Mater.* **2001**, *13*, 140. (b) Korgel, B. A.; Fullam, S.; Connolly, S.; Fitzmaurice, D. *J. Phys. Chem. B* **1998**, *102*, 8379. (c) Maoz, R.; Frydman, E.; Cohen, S. R.; Sagiv, J. *Adv. Mater.* **2000**, *12*, 424. (d) Pan, Z. Y.; Liu, X. J.; Zhang, S. Y.; Shen, G. J.; Zhang, L. G.; Lu, Z. H.; Liu, J. Z. *J. Phys. Chem. B* **1997**, *101*, 9703. (e) Vossmeyer, Deionno, T. E.; Heath, J. R. *Angew. Chem.* **1997**, *109*, 1123; *Angew. Chem., Int. Ed. Engl.* **1997**, *36*, 1080.

(2) (a) Morales, A. M.; Lieber, C. M. *Science* **1998**, *279*, 208. (b) Han, W. Q.; Fan, S. S.; Li, Q. Q.; Hu, Y. D. *Science* **1997**, *277*, 1287. (c) Alivisatos, A. P. *Science* **1996**, *271*, 933. (d) Dai H.; Wong, E. W.; Lu, Y. Z.; Fan, S.; Lieber, C. M. *Nature* **1995**, *375*, 769. (e) Feldman, C.; Jungk, H. O. *Angew. Chem.* **2001**, *13*, 372; *Angew. Chem., Int. Ed.* **2001**, *40*, 359. (f) Saito, S. *Science* **1997**, *278*, 77. (g) Yu, H.; Gibbons, P. C.; Kelton, K. F.; Bubro, W. E. *J. Am. Chem. Soc.* **2001**, *123*, 359.

(3) (a) Routkevitch, D.; Bigioni, T.; Moskovits, M.; Xu, J. M. *J. Phys. Chem.* **1996**, *100*, 14037. (b) Cao, H.; Xu, Z.; Sang, H.; Sheng, D.; Tie, C. *Adv. Mater.* **2001**, *13*, 121. (c) Huang, M. H.; Mao, S.; Yan, H.; Wu, Y.; Kind, H.; Weber, E.; Russo, R.; Yang, P. *Science* **2001**, *292*, 1897.

(4) (a) Thackeray, M. M. *Prog. Solid State Chem.* **1997**, *25*, 1. (b) Armstrong, A. R.; Bruce, P. G. *Nature* **1996**, *381*, 499. (c) Ammundsen, B.; Paulsen, J. *Adv. Mater.* **2001**, *13*, 943.

(5) (a) Golden, D. C.; Chen, C. C.; Dixon, J. B. *Science* **1986**, *231*, 717−719. (b) DeGuzman, R. N.; Shen, Y. F.; Neth, E. J.; Suib, S. L.; O'Young, C. L.; Levine, S.; Newsam, J. M. *Chem. Mater.* **1994**, *6*, 815−821. (c) Shen, Y. F.; Zerger, R. P.; Suib, S. L.; Mecurdy, L.; Potter, D. I.; O'Young, C. L. *Science* **1993**, *5*, 260, 511−515.

(6) (a) Wang, X.; Li, Y. D. *J. Am. Chem. Soc.* **2002**, *124*, 2880. (b) Wang, X.; Li, Y. *Chem. Commun.* **2002**, *124*, 764.

(7) Xiong, Y. J.; Xie, Y.; Li, Z. Q.; Wu, C. Z. *Chem.—Eur. J.* **2003**, *9*, 1645.

(8) Kazou, N. *Infrared and Raman Spectra of Inorganic and Coordination Compounds*; Wiley: New York, 1977.

(9) Julien, C.; Massot, M.; Rangan, S.; Lemal, M.; Guyomard, D. J. *Raman Spectrosc.* **2002**, *33*, 223.

(10) (a) Chen, X.; Sun, X.; Li, Y. *Inorg. Chem.* **2002**, *41*, 4524. (b) Li, Y.; Li, X.; He, R. *J. Am. Chem. Soc.* **2002**, *124*, 1411.

(11) Wang, X.; Li, Y. *Chem.—Eur. J.* **2003**, *9*, 300.

(12) (a) Gates, B.; Mayers, B.; Cattle, B.; Xia, Y. *Adv. Funct. Mater.* **2002**, *12*, 219. (b) Gates, B.; Yin, Y.; Xia, Y. *J. Am. Chem. Soc.* **2000**, *122*, 12582.

(13) (a) Sun, Y.; Xia, Y. *Adv. Mater.* **2002**, *14*, 833. (b) Sun, Y.; Gates, B.; Mayers, B.; Xia, Y. *Nano Lett.* **2002**, *2*, 165.

(14) Qian, Y. T. *Introduction to Crystallography*; University of Science and Technology Press: Hefei, China, 1999 (in Chinese).